Supplementary Material for

Visible-light-driven BNQDs/$BiVO_4$ material with enhanced photocatalytic activities for naproxen degradation and kinetic insights

Minghao Liu [a], Yongxian Chen [a], Daguang Li [a], Shoubin Huang [a], Zheng Fang [a], Zhenjun Xiao [a], Haijin Liu [b], Ping Chen [a,], Wenying Lv [a], Guoguang Liu [a,*].*

[a] Guangdong Key Laboratory of Environmental Catalysis and Health Risk Control, Guangdong-HongKong-Macao Joint Laboratory for Contaminants Exposure and Health, School of Environmental Science and Engineering, Guangdong University of Technology, Guangzhou, 510006, China

[b] School of Environment, Henan Normal University, Key Laboratory for Yellow River and Huaihe River Water Environment and Pollution Control, Xinxiang 453007, China

*** Corresponding Author**: Guoguang Liu and Ping Chen

E-mail: liugg615@163.com; 15018448140@163.com

Tel: +86-20-39322547

Fax: +86-20-39322548

Table. S1. Efficiency of different processes for removing NPX in literature.

Photocatalyst	Dosage	Initial NPX concentration	k_{obs} (min^{-1})	Photocatalytic performance	Ref.
0.3BQBVO	0.5 g/L	15 mg/L	0.0356	87.28% (60 min)	Our work
$ZnFe_2O_4$@TiO_2/Cu	0.04 g/L	10 mg/L		79.8% (120 min)	[1]
SnO_2/AC nanocomposite	0.03 g/L	5 mg/L		94% (240 min)	[2]
Bi_2MoO_6–BDD		15 mg/L		85% (360 min)	[3]
ZnO/TiO_2/Ag_2Se		5 mg/L	0.0126	100% (210 min)	[4]
Bi-TNB	1.0 g/L	0.25 mg/L	0.0021	35.43% (60 min)	[5]
MoS_2/N-TiO_2/Ti		12 mg/L	0.0224	77.8% (150 min)	[6]
BSW	1.0 g/L	10 mg/L	0.0067	76.5% (180 min)	[7]

Text. S1. Sample characterization

The crystalline structures of the photocatalysts were identified by Powder X-ray Diffraction (XRD, Rigaku SmartLab 9 kW), equipped with Cu Kα radiation (λ = 0.15418 nm) in the 2θ range. The microscopic morphologies of the samples were observed via scanning electron microscopy (SEM, Hitachi Regulus8100) and a transmission electron microscope (TEM, FEI Talos F200x). The X-ray photoelectron spectroscopy (XPS) measurements were obtained using a Thermo Scientific K-Alpha. The UV–visible diffuse reflectance spectra (UV-Vis DRS) with a wavelength range of 200–800 nm were obtained using a Shimadzu UV-3600 Plus UV–visible spectrophotometer. Using an ESR (JEOL JES-FA200) test, the generation of various active free radical species under visible light irradiation were obtained. The photoluminescence (PL) spectra and transient photoluminescence attenuation spectrum were studied with a transient fluorescence spectrometer (Hitachi F-4600). Raman spectroscopy (Horiba LabRAM HR Evolution) was used to measure the chemical composition of the samples.

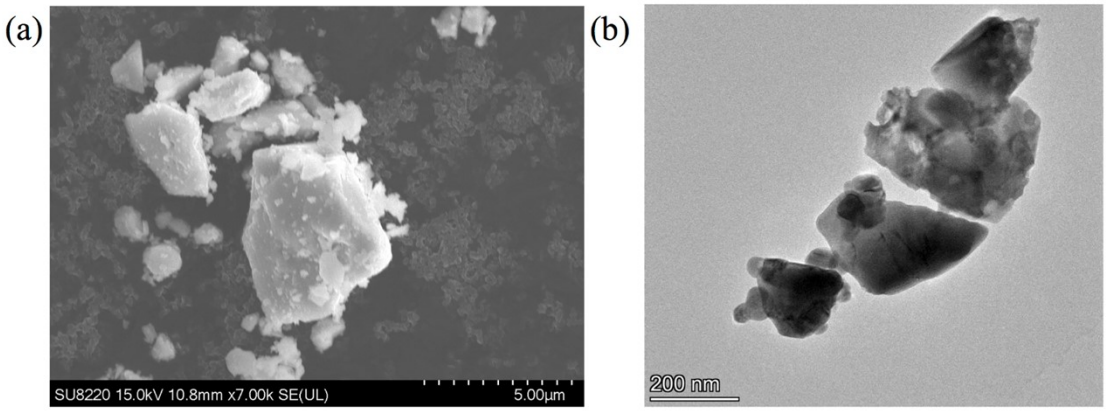

Fig. S1. (a) SEM image and (b) TEM image of BVO.

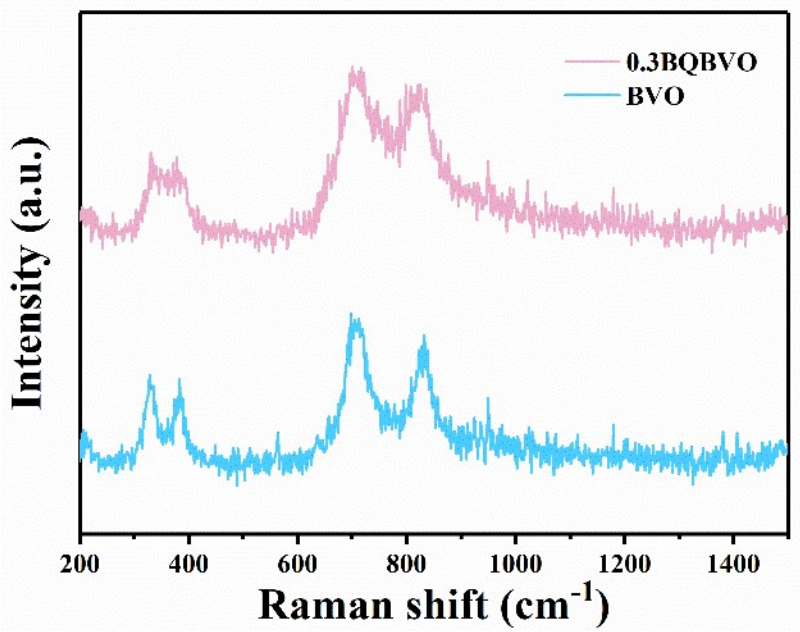

Fig. S2. Raman spectra of BVO and 0.3BQBVO.

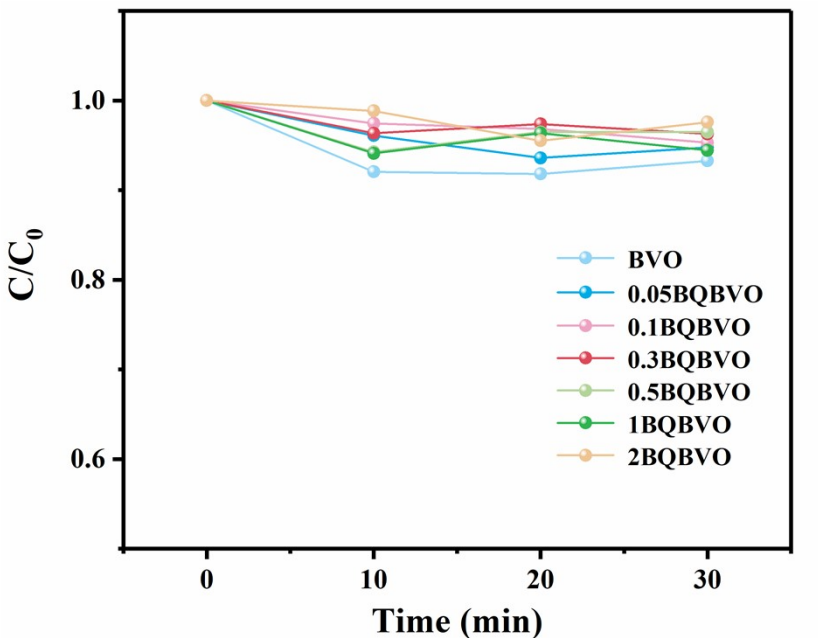

Fig. S3. The adsorption for NPX of the samples in the darkness.

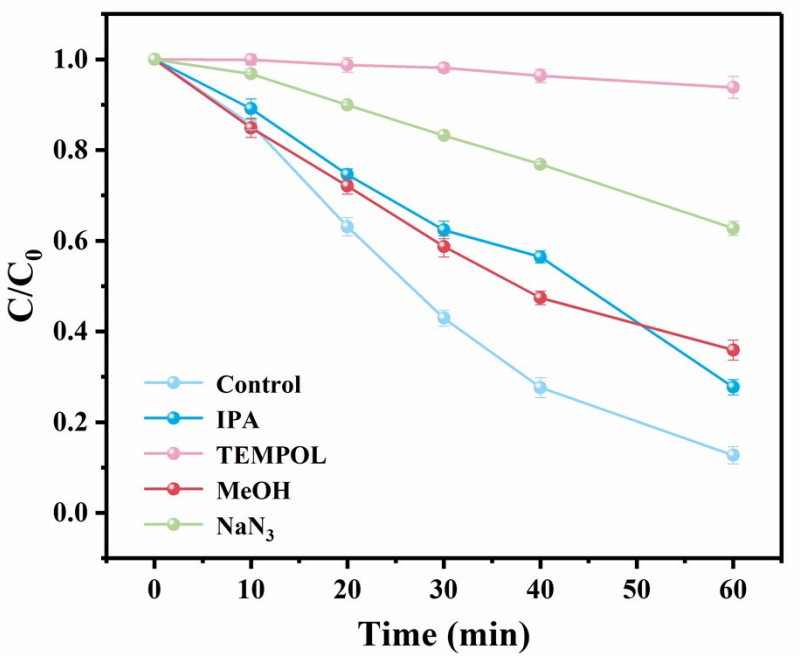

Fig. S4. Photocatalytic activity of 0.3BQBVO photocatalytic for NPX degradation under visible light with the addition of different scavengers.

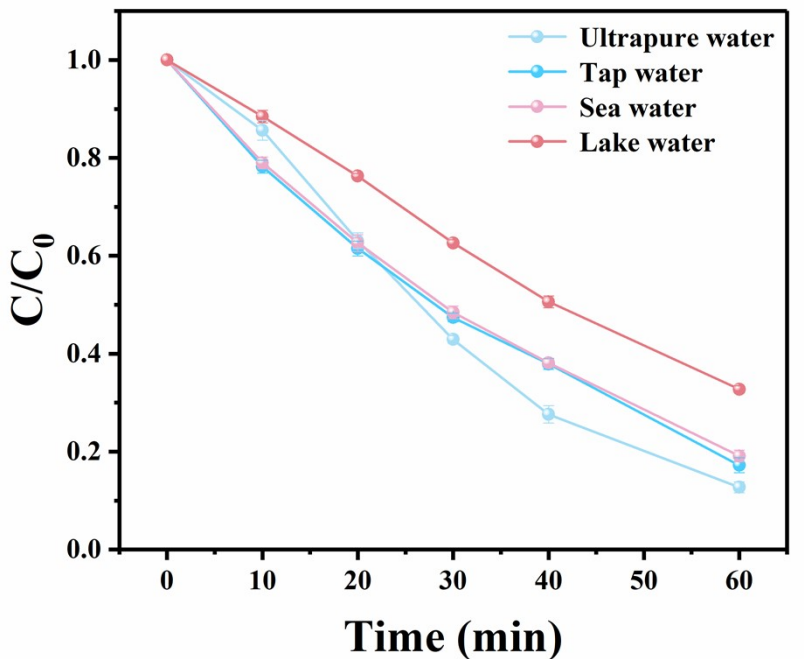

Fig. S5. Photoactivity under diverse aqueous matrices. (NPX:10 mg/L; Powder dosage: 500 mg/L).

Table. S2. Transformation products from the photocatalytic degradation of NPX under visible light irradiation. Products, labeled P1-P9 were identified by UPLC-Q-TOF MS.

serial number	Rt / min	m/z	Molecular formula	Probable structure
NPX	13.71	230	$C_{14}H_{14}O_3$	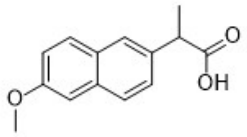
P1	14.20	186	$C_{13}H_{14}O$	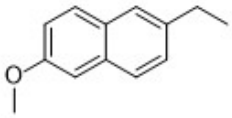
P2	6.10	218	$C_{13}H_{14}O_3$	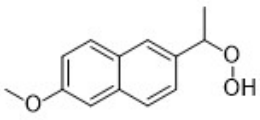
P3	13.45	184	$C_{13}H_{12}O$	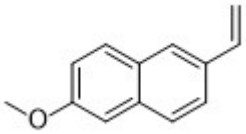
P4	13.88	170	$C_{12}H_{10}O$	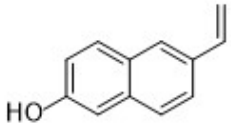
P5	14.62	202	$C_{13}H_{14}O_2$	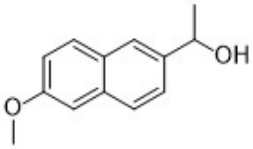
P6	13.38	200	$C_{13}H_{12}O_2$	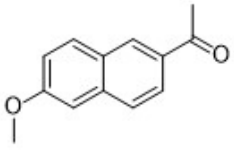
P7	13.29	158	$C_{11}H_{10}O$	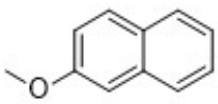

P8	7.67	216	$C_{13}H_{12}O_3$	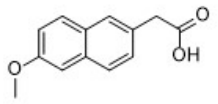
P9	8.26	244	$C_{15}H_{16}O_3$	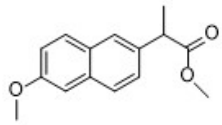

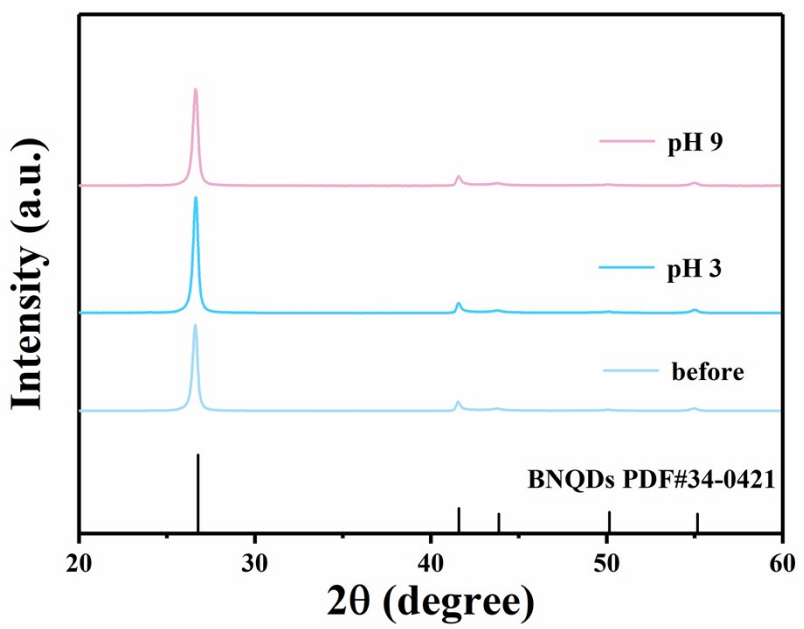

Fig. S6. XRD patterns of BNQDs, prior to and following photocatalytic experiments conducting in aqueous solutions with pH of 3 and 9.

References

1. N. Ahmadpour, M. H. Sayadi, S. Sobhani and M. Hajiani, A potential natural solar light active photocatalyst using magnetic $ZnFe_2O_4$@ TiO_2/Cu nanocomposite as a high performance and recyclable platform for degradation of naproxen from aqueous solution, *Journal of cleaner production*, 2020, **268**, 122023.
2. S. Begum and M. Ahmaruzzaman, Biogenic synthesis of SnO_2/activated carbon nanocomposite and its application as photocatalyst in the degradation of naproxen, *Applied Surface Science*, 2018, **449**, 780-789.
3. X. Zhao, J. Qu, H. Liu, Z. Qiang, R. Liu and C. Hu, Photoelectrochemical degradation of anti-inflammatory pharmaceuticals at Bi_2MoO_6–boron-doped diamond hybrid electrode under visible light irradiation, *Applied Catalysis B: Environmental*, 2009, **91**, 539-545.
4. K. Changanaqui, H. Alarcon, E. Brillas and I. Sires, Blue LED light-driven photoelectrocatalytic removal of naproxen from water: Kinetics and primary by-products, *Journal of Electroanalytical Chemistry*, 2020, **867**, 114192.
5. G. Fan, R. Ning, J. Luo, J. Zhang, P. Hua, Y. Guo and Z. Li, Visible-light-driven photocatalytic degradation of naproxen by Bi-modified titanate nanobulks: Synthesis, degradation pathway and mechanism, *Journal of Photochemistry and Photobiology A: Chemistry*, 2020, **386**, 112108.
6. M. Sheydaei, A. Haseli, B. Ayoubi-Feiz and V. Vatanpour, MoS_2/N-TiO_2/Ti mesh plate for visible-light photocatalytic ozonation of naproxen and industrial wastewater: comparative studies and artificial neural network modeling, *Environmental Science and Pollution Research*, 2021, 1-15.
7. C. Regmi, Y. K. Kshetri, R. P. Pandey and S. W. Lee, Visible-light-driven S and W co-doped dendritic $BiVO_4$ for efficient photocatalytic degradation of naproxen and its mechanistic analysis, *Molecular Catalysis*, 2018, **453**, 149-160.